THE JOURNAL OF PHYSICAL CHEMISTRY A
A JOURNAL OF THE AMERICAN CHEMICAL SOCIETY

pubs.acs.org/JPCA Article

Reducing the Cost of TD-CI Simulations of Strong Field Ionization

Published as part of The Journal of Physical Chemistry A special issue "Gustavo Scuseria Festschrift".

Andrew S. Durden and H. Bernhard Schlegel*

Cite This: https://doi.org/10.1021/acs.jpca.4c01732 Read Online

ACCESS | Metrics & More | Article Recommendations

ABSTRACT: Strong field ionization of molecules by intense laser pulses can be simulated by time-dependent configuration interaction (TD-CI) with a complex absorbing potential (CAP). Standard molecular basis sets need to be augmented with several sets of diffuse functions for effective interaction with the CAP. This dramatically increases the number of configurations and the cost of the TD-CI simulations as the size of the molecules increases. The cost can be reduced by making use of spin symmetry and by employing an orbital energy cutoff to limit the number of virtual orbitals used to construct the excited configurations. Greater reductions in the number of virtual orbitals can be obtained by examining their interaction with the absorbing potential during simulations and their contributions to the strong field ionization rate. This can be determined from the matrix elements of the absorbing potential and the TD-CI coefficients from test simulations. Compared to a simple 3 hartree cutoff in the orbital energies, these approaches reduce the number of virtual orbitals by 20−35% for neutral molecules and 5−10% for cations. As a result, the cost of simulations is reduced by 35−60% for neutral molecules. The number of virtual orbitals needed can also be estimated by second-order perturbation theory without the need for test simulations. The number of virtual orbitals can be reduced further by adapting orbitals to the laser field using natural orbitals derived from test simulations. This is particularly effective for cations, yielding reductions of more than 20%.

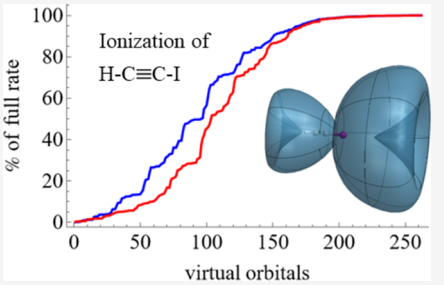

INTRODUCTION

In attosecond spectroscopy and strong field chemistry, ultrashort intense laser pulses (typically a few femtoseconds and 10^{14} W cm^{-2}) are used to probe the dynamics of electrons on their natural time scale. Because the electron density can be strongly distorted under these conditions, time-independent and perturbative approaches are not suitable. Instead, strong field ionization requires simulations of electron dynamics by quantum-mechanical propagation in the presence of the intense laser field. Simulations of electron dynamics and ionization in strong laser fields have been discussed in a number of recent reviews.[1−6] Accurate solutions for one- and two-electron systems can be obtained by solving the time-dependent Schrödinger equation. Because this is not practical for larger systems, various approximate methods have been developed. The single active electron (SAE) approximation and the strong field approximation (SFA) are frequently used for multielectron systems. Orientation-dependent ionization rates can be modeled by molecular Ammosov−Delone−Krainov (MO-ADK) model[7] and weak-field asymptotic theory (WFAT).[8] More detailed descriptions of electron dynamics require numerical simulations (see refs 1−6 for recent reviews). Two of the methods that have been used successfully for propagating the electronic structure to model strong field ionization in multielectron polyatomic systems are time-dependent configuration interaction (TD-CI)[9−16] and real-time integration of time-dependent density functional theory (rt-TD-DFT).[17−23] To model ionization with these approaches, a complex absorbing potential is used to remove the outgoing electron density.[24−26] Both rt-TDDFT and TD-CI simulations are very demanding in terms of computer resources. In previous work we have developed an efficient TD-CI approach for studying strong field ionization and have applied it to a number of systems.[15,16,27−37] In the present paper, we explore some approaches to reducing the cost of TD-CI simulations of strong field ionization. These include using spin symmetry, removing high-energy excited configurations that are not accessed in a simulation, and reducing the number of virtual orbitals by eliminating those that do not make a significant contribution in the simulations.

METHODS

In the TD-CI approach, the electronic wavefunction is propagated with the time-dependent Schrödinger equation:

Received: March 15, 2024
Revised: July 7, 2024
Accepted: August 6, 2024

$$i\hbar\frac{\partial}{\partial t}\Psi(t) = \hat{\mathbf{H}}(t)\Psi(t) = [\hat{\mathbf{H}}_{el} - \boldsymbol{\mu}\cdot\mathbf{E}(t) - i\hat{\mathbf{V}}^{abs}]\Psi(t) \tag{1}$$

where $\hat{\mathbf{H}}_{el}$ is the field-free, time-independent electronic Hamiltonian and the interaction with the electric field of an intense laser pulse is treated in the semiclassical dipole approximation, where $\hat{\boldsymbol{\mu}}$ is the dipole moment operator and $\mathbf{E}$ is the electric field.

The absorbing potential $\hat{\mathbf{V}}^{abs}$ surrounds the molecule starting at a distance of about 10−15 bohr and removes the outgoing part of the wavefunction, thereby simulating ionization. The absorbing potential for the molecule is constructed from spherical potentials centered on each atom. In our previous work,[15] the potential on atom C was written in terms of the distance from the nucleus, $r_C = |\mathbf{r} - \mathbf{C}|$, and started at R_A, rose quadratically to $(R_A + R_B)/2$, turned over quadratically to R_B, and was constant (V_{max}) beyond R_B:

$$\hat{V}_C^{abs}(r_C) = \begin{cases} 0 & r_C \le R_A \\ 2V_{max}\left(\dfrac{r_C - R_A}{R_B - R_A}\right)^2 & R_A \le r_C \le \dfrac{R_A + R_B}{2} \\ V_{max} - 2V_{max}\left(\dfrac{R_B - r_C}{R_B - R_A}\right)^2 & \dfrac{R_A + R_B}{2} \le r_C \le R_B \\ V_{max} & r_C \ge R_B \end{cases} \tag{2}$$

In the present work, the absorbing potential on an atom is written in terms of a $\sin^2$ function of the distance from the atom:[38]

$$\hat{V}_C^{abs}(r_C) = V_{max}\sin^2\left[\frac{\pi}{2}\left(\frac{r_C - R_A}{R_B - R_A}\right)\right], \quad R_A \le r_C \le R_B \tag{3}$$

The absorbing potential for the molecule is equal to the minimum of the values of the atomic absorbing potentials:[15]

$$\hat{\mathbf{V}}^{abs}(\mathbf{r}) = \min(\hat{V}_1^{abs}, \hat{V}_2^{abs}, ..., \hat{V}_{N_{atoms}}^{abs}) \tag{4}$$

This has also been termed a Voronoi absorbing potential.[26]

Typical values used in our previous work are R_A = 3.5 times the van der Waals radius for each atom (so that the absorbing potential starts well beyond the Coulomb well), R_B = 12 times the van der Waals radius (so that the rise in the absorbing potential is gradual enough to minimize any reflection), and V_{max} = 10 hartree (so that the potential is strongly absorbing and the integrals remain finite).

In the TD-CI approach, the wavefunction is written as a linear combination of time-dependent coefficients with time-independent states of the field-free Hamiltonian, Ψ_s:

$$\Psi(t) = \sum_s C_s(t)\Psi_s \tag{5}$$

For single ionization of a neutral molecule to a cation, a wavefunction consisting of the ground state and all singly excited configurations (CIS) is suitable:

$$\Psi(t) = c_0(t)\psi_0 + \sum_{i,a} c_i^a(t)\psi_i^a \tag{6}$$

where ψ_i^a are singly excited determinants and i, j, etc. and a, b, etc. are indices for the occupied and virtual molecular spin-orbitals, respectively.

For ionization of a cation to a dication, a spin-unrestricted wavefunction could be used, but this would treat the α and β spin-orbitals differently. This problem can be overcome by using a CISD-IP wavefunction.[39] The wavefunction is constructed using the molecular orbitals of the closed-shell system and includes singly ionized determinants, ψ_x, and singly excited, singly ionized determinants, ψ_{xi}^a:

$$\Psi(t) = \sum_x c_x(t)\psi_x + \sum_{x,i,a} c_{xi}^a(t)\psi_{xi}^a \tag{7}$$

where x indicates the ionized molecular spin-orbitals. The ionizations generate the ground and excited states of the cation, and the single excitations serve to improve the energies of these cation states. As a result, the energies of the cation states will depend slightly on the number of virtual orbitals used to construct the singly excited, singly ionized determinants.

The ionization rate is taken as the rate of decrease in the norm squared of the wavefunction. Using the time-dependent Schrödinger equation, the rate can be related to the expectation value of the absorbing potential:

$$\begin{aligned} \text{rate}(t) &= -\frac{d\langle\Psi(t)|\Psi(t)\rangle}{dt} \\ &= 2\langle\Psi(t)|\hat{\mathbf{V}}^{abs}|\Psi(t)\rangle \\ &= 2\sum_{r,s} C_r^*(t)C_s(t)\langle\Psi_r|\hat{\mathbf{V}}^{abs}|\Psi_s\rangle \end{aligned} \tag{8}$$

where r and s are indices for configurations. For simplicity, the CIS wavefunction is used in the following equations, but these can be easily extended to CISD-IP. In terms of determinants, the ionization rate is

$$\begin{aligned} \text{rate}(t) = 2[&c_0^*(t)c_0(t)\langle\psi_0|\hat{\mathbf{V}}^{abs}|\psi_0\rangle + \sum_{i,a} c_i^{a*}(t)c_0(t)\langle\psi_i^a|\hat{\mathbf{V}}^{abs}|\psi_0\rangle \\ &+ \sum_{j,b} c_0^*(t)c_j^b(t)\langle\psi_0|\hat{\mathbf{V}}^{abs}|\psi_j^b\rangle + \sum_{i,j,a,b} c_i^{a*}(t)c_j^b(t)\langle\psi_i^a|\hat{\mathbf{V}}^{abs}|\psi_j^b\rangle] \end{aligned} \tag{9}$$

The rate can also be written in terms of the density matrix and the absorbing potential in the basis of the molecular orbitals, ϕ_p:

$$\text{rate}(t) = 2\sum_{p,q}^{all} \rho_{pq}(t)\langle\phi_p|\hat{\mathbf{V}}^{abs}|\phi_q\rangle \tag{10}$$

where $\rho_{pq}(t)$ is the time-dependent one-particle density matrix derived from the CI wavefunction and indices p and q run over all occupied and virtual orbitals. This form is also applicable to rt-TD-DFT.

Propagation of the time-dependent wavefunction for simulating strong field dynamics comes with a number of challenges. The absorbing potential needs to be placed sufficiently far from the Coulomb well of the molecule to minimize the effect on the field-free electronic dynamics. To support the wavefunction outside of the Coulomb well and to interact with the absorbing potential, a large number of diffuse functions need to be added to the basis set. Typically, 200 to 400 diffuse functions are needed, leading to a large number of virtual orbitals and a larger number of excited configurations

https://doi.org/10.1021/acs.jpca.4c01732
J. Phys. Chem. A XXXX, XXX, XXX−XXX

with a wide range of energies. Placing the absorbing potential further away would increase the number of diffuse functions needed. Using 3.5 times the van der Waals radius as the start of the absorbing potential seems to be a good compromise for strong field ionization with laser intensities of around 10^{14} W cm^{-2}. The number of occupied orbitals can often be limited to four to six highest-energy occupied orbitals. Since the ionization rate depends on the inverse of the exponential of the ionization potential, the contribution of lower-energy orbitals to the ionization rate is negligible

For typical strong field ionization studies, numerous simulations of 20−50 fs are needed (e.g., different pulse shapes, intensities, and directions, different delay times in pump−probe simulations, etc.). Because of the strong fields and the wide range of energies of the excited configurations, small time steps are required for the propagation. We have chosen to propagate the wavefunction with the exponential of the Hamiltonian, since this unitary transformation is very stable and allows for larger time steps. Typically, a time step of 0.05 au = 1.2 as can be used. Reducing the time step by a factor of 2 changes the ionization rate by less than 0.02% for typical simulations. For larger molecules, other propagators that do not involve exponentiation may be more suitable, but at the cost of a much smaller time step. There is little to be gained in computing $\boldsymbol{\sigma} = \mathbf{HC}$ directly, since $\mathbf{H}$ is a full matrix (i.e., no sparsity). In any case, the cost of the propagation will depend on the total number of configurations, which depends primarily on the number of virtual orbitals.

The exponential of the Hamiltonian can be obtained via a Trotter factorization with components depending on the field-free Hamiltonian, the absorbing potential, and the dipole moment matrix:

$$\Psi(t + \Delta t) = e^{-i\hat{\mathbf{H}}\Delta t}\Psi(t)$$

$$\begin{aligned}\mathbf{C}(t + \Delta t) &= e^{-i\hat{\mathbf{H}}_{el}\Delta t/2}e^{-\hat{\mathbf{V}}^{abs}\Delta t/2}e^{iE(t+\Delta t/2)\hat{\mathbf{D}}\Delta t} \\ &\quad e^{-\hat{\mathbf{V}}^{abs}\Delta t/2}e^{-i\hat{\mathbf{H}}_{el}\Delta t/2}\mathbf{C}(t) \\ &= e^{-i\hat{\mathbf{H}}_{el}\Delta t/2}\mathbf{U}^{T}e^{iE(t+\Delta t/2\mathbf{d}\Delta t)}\mathbf{U}e^{-i\hat{\mathbf{H}}_{el}\Delta t/2}\mathbf{C}(t)\end{aligned} \quad (11)$$

This requires some initial diagonalizations but avoids the exponentiation of a full matrix at every time step. The field-free Hamiltonian is time-independent, and it can be diagonalized once at the beginning of the simulation. By working in the eigenbasis of the field-free Hamiltonian, the exponential of the field-free Hamiltonian, $\exp(-i\mathbf{H}_{el}\Delta t/2)$, is a diagonal matrix and is easy to calculate. Because the absorbing potential is time-independent, $\exp(-\mathbf{V}^{abs}\Delta t/2)$ needs to be calculated only once. The calculation of $\exp(iE(t + \Delta t/2)\mathbf{D}\Delta t)$ would require exponentation of a full matrix at each time step. However, by diagonalizing $\mathbf{D} = \mathbf{W}^{T}\mathbf{dW}$ once at the beginning of the simulation and working in the eigenbasis of $\mathbf{D}$, the contribution reduces to an easy-to-calculate exponential of a time-dependent diagonal matrix, $\exp(iE(t + \Delta t/2)\mathbf{d}\Delta t)$. The product $\mathbf{U} = \exp(-\mathbf{V}^{abs}\Delta t/2)\mathbf{W}^{T}$ is formed once at the beginning of the propagation. Thus, all of the N^3 steps need to be done only once at the beginning and can be reused for many subsequent simulations. A propagation step for a linearly polarized pulse with fixed nuclear positions scales as N^2 and involves two full matrix−vector multiplications ($\mathbf{U}$ and $\mathbf{U}^{T}$) and three diagonal matrix−vector multiplications ($\exp(-i\mathbf{H}_{el}\Delta t/2)$ and $\exp(iE(t + \Delta t/2)\mathbf{d}\Delta t)$). Propagation for a circularly polarized pulse with fixed nuclei also scales as N^2 and involves two field directions. This requires four full matrix−vector multiplications and five diagonal matrix−vector multiplications. In typical strong field studies for the molecules that we have studied so far, the total CPU time for the propagations for the various laser pulse parameters significantly exceeds the initial diagonalization and exponentiation. For larger molecules, alternate propagation schemes can be considered that avoid explicit diagonalization and exponentials of various matrices. However, such approaches would typically require much smaller time steps to achieve the same accuracy and stability.

The $\mathbf{V}^{abs}$ integrals needed for the TD-CI simulation were calculated with a development version of the Gaussian software suite.[40] The aug-cc-pVTZ basis set was used for H, C, and O;[41−43] the aug-cc-pVTZ-PP basis set with pseudopotential was used for iodine.[44] To ensure adequate interaction with the absorbing potential and to describe the electron dynamics during the ionization process, additional diffuse functions were placed on each atom. For CH_3Br and HCCI, this set of basis functions consisted of four s functions (exponents of 0.0256, 0.0128, 0.0064, and 0.0032), four p functions (exponents of 0.0256, 0.0128, 0.0064, and 0.0032), five d functions (exponents of 0.0512, 0.0256, 0.0128, 0.0064, and 0.0032), and two f functions (exponents of 0.0256 and 0.0128).[15,28] For propiolic acid and benzene, a smaller set of diffuse basis functions was added, consisting of three s functions (exponents of 0.0256, 0.0128, and 0.0064), two p functions (exponents of 0.0256 and 0.0128), three d functions (exponents of 0.0512, 0.0256, and 0.0128), and one f function (exponent of 0.0256). The large number of diffuse functions leads to some near linear dependencies; these are removed in the Gaussian code before the integrals are calculated. Some of the highest-energy virtual orbitals (15−40 orbitals) are also removed because they do not contribute to the ionization rate but can cause instabilities in the propagation. The spherical absorbing potential on each atom was chosen to start at R_A = 3.5 times the van der Waals radius and rise to V_{max} = 12 hartree at R_B = 10 times the van der Waals radius used in the Gaussian code (this corresponds to R_A = 14.882, 13.853, 12.735, 11.575, and 9.544 bohr and R_B = 51.023, 47.496, 43.664, 39.684, and 32.723 bohr for I, Br, C, O, and H, respectively; 1 bohr = 0.529177 Å). The TD-CI simulations were carried out with an external Fortran95 code. Mathematica[45] was used to analyze the simulations and plot the results.

a. Computational Effort Required for Simulation of Strong Field Ionization Rates with TD-CI. The diagonalizations and matrix multiplications in the setup for a TD-CI simulation require $O(N^3)$ work, while the propagation requires N_{steps} $O(N^2)$ work, where N is the number of configurations and N_{steps} is the number of propagation steps. The number of occupied valence orbitals, O, is typically four to six, and the number of virtual orbitals, V, can be 200−600. N ranges from OV for TD-CIS for a closed-shell singlet up to approximately $3O^2V$ for TD-CISD-IP for a radical cation. The cost can be reduced by decreasing N by discarding some of the highest-energy configurations (previously, a simple energy cutoff was used, typically 10 hartree). Alternatively, N can be reduced by decreasing the number of virtual orbitals used to construct the excited configurations. In earlier studies, a simple energy cutoff in the orbital energies was used to select the virtual orbitals (typically 3 hartree). A more rational approach can be developed to discard configurations and orbitals based on their contribution to the ionization rate. A number of methods

https://doi.org/10.1021/acs.jpca.4c01732
J. Phys. Chem. A XXXX, XXX, XXX−XXX

to reduce the cost of TD-CI simulations are outlined below and are validated by comparison to simulations with the full complement of configurations and orbitals. The use of spin symmetry is the most obvious, while other methods described below aim to reduce the number of states and/or orbitals employed in the simulation.

b. Reducing the Number of States by Using Spin Symmetry. The TD-CI approach for strong field ionization outlined above is presented in terms of an unrestricted spin-orbital formalism to simplify the notation. This is appropriate for open-shell molecules and for cases where spin−orbit coupling is needed. For TD-CIS simulations of ionization of closed-shell neutral molecules without spin−orbit coupling, the excitations can clearly be restricted to singlet states since transitions to triplet states are forbidden. This reduces the number of states by a factor of 2 compared to spin-unrestricted TD-CIS. Likewise, for CISD-IP simulations of ionization of cations derived from a closed-shell neutral molecule without spin−orbit coupling, the ionization rates for α and β cations are equal. By restricting the ionization to β cations but including excitations of both α and β electrons, the total number of states is also decreased by a factor of 2. A factor of 2 reduction in the number of states reduces the CPU cost of the propagation by a factor of 4 and the preliminary work involving diagonalization and matrix multiplications by a factor of 8. However, if spin−orbit coupling is needed, the α and β spin-orbitals interact, and the full complement of α and β states must be included.

c. Reducing the Number of States Based on Their Contribution to the Ionization Rate. In a typical TD-CI simulation, the wavefunction includes all CIS or CISD-IP configurations that can be constructed from a range of occupied and virtual orbitals. Since the strong field ionization decreases exponentially with the ionization potential, only a limited number of occupied valence orbitals need to be included. The number of virtual orbitals required depends on the distance to the absorbing potential. Typically, several sets of diffuse functions are added to the basis set to support the wavefunction outside the molecular Coulomb well and to interact with the absorbing potential. Some of the resulting virtual orbitals overlap well with the absorbing potential, whereas others are higher in energy and contribute little to the strong field ionization rate because they do not interact significantly with the absorbing potential. In prior work, we used a simple energy cutoff in the orbital energies (e.g., 3 hartree) to choose the virtual orbitals to include in the simulation. This range of occupied and virtual orbitals is used to construct the CIS or CISD-IP configurations for the ground and excited states of the field-free Hamiltonian.

A better approach is to discard states based on their interaction with the absorbing potential during the simulation as determined by their contribution to the ionization rate. For states ordered in increasing energy, the ionization rate calculated using states up to $\psi_{s_{max}}$ is

$$\text{rate}(t, s_{\max}) = 2\sum_{r,s}^{s_{\max}} C_r^*(t)C_s(t)\langle\Psi_r|\hat{\mathbf{V}}^{\text{abs}}|\Psi_s\rangle \tag{12}$$

where s_{max} is chosen so that rate(t, s_{max}) is suitably close to the full rate when all excited states are included at each step in the simulation. For illustrative purposes in the present work, the cutoff is chosen to yield 99% of the full rate (looser cutoffs might be needed to make larger simulations practical). This maximum number of configurations reduces the $O(N^2)$ work needed for the propagation but not the $O(N^3)$ work needed for the initial diagonalization of the Hamiltonian and exponentiation of the absorbing potential. The $O(N^3)$ work may be the limiting factor for large simulations. Furthermore, the CI coefficients used to determine the cutoff need to be obtained from test simulations with the full set of excited states.

d. Reducing the Number of Canonical Molecular Orbitals Based on Their Contribution to the Ionization Rate. To decrease the initial $O(N^3)$ work, the number of occupied and virtual orbitals used in the simulations needs to be reduced. The interaction of individual orbitals with the absorbing potential during a simulation and their contribution to the ionization rate can be seen by writing the total ionization rate in terms of determinants (eq 9). If the number of virtual orbitals is limited to a_{max}, the rate is

$$\begin{aligned}\text{rate}(t, a_{\max}) = 2[&c_0^*(t)c_0(t)\langle\psi_0|\hat{\mathbf{V}}^{\text{abs}}|\psi_0\rangle \\ &+ \sum_{a}^{a_{\max}}\sum_{i,a}^{\text{all}} c_i^{a*}(t)c_0(t)\langle\psi_i^a|\hat{\mathbf{V}}^{\text{abs}}|\psi_0\rangle \\ &+ \sum_{b}^{a_{\max}}\sum_{j}^{\text{all}} c_0^*(t)c_j^b(t)\langle\psi_0|\hat{\mathbf{V}}^{\text{abs}}|\psi_j^b\rangle \\ &+ \sum_{a,b}^{a_{\max}}\sum_{i,j}^{\text{all}} c_i^{a*}(t)c_j^b(t)\langle\psi_i^a|\hat{\mathbf{V}}^{\text{abs}}|\psi_j^b\rangle]\end{aligned} \tag{13}$$

where a_{max} can be chosen so that rate(t, a_{max}) for each step in the simulation is 99% of the rate when the full set of virtual orbitals is included. Note that the individual terms in the sums may be positive or negative. Furthermore, the same a_{max} might be used for different shapes, intensities, and polarization directions of the laser pulse. Thus, a more robust approach is to sum the absolute values of the most relevant terms and choose a_{max} such that the following ratio is 0.99:

$$\text{ratio}(t, a_{\max}) = \frac{\sum_{a}^{a_{\max}}\sum_{i}^{\text{all}}|c_i^{a*}(t)c_0(t)\langle\psi_i^a|\hat{\mathbf{V}}^{\text{abs}}|\psi_0\rangle| + \sum_{a}^{a_{\max}}\sum_{i,j,b}^{\text{all}}|c_i^{a*}(t)c_j^b(t)\langle\psi_i^a|\hat{\mathbf{V}}^{\text{abs}}|\psi_j^b\rangle|}{\sum_{a}^{\text{all}}\sum_{i}^{\text{all}}|c_i^{a*}(t)c_0(t)\langle\psi_i^a|\hat{\mathbf{V}}^{\text{abs}}|\psi_0\rangle| + \sum_{a}^{\text{all}}\sum_{i,j,b}^{\text{all}}|c_i^{a*}(t)c_j^b(t)\langle\psi_i^a|\hat{\mathbf{V}}^{\text{abs}}|\psi_j^b\rangle|} \tag{14}$$

In the Results and Discussion, this is termed the canonical molecular orbital (CMO) method to contrast it with the natural orbital (NO) method discussed below. Like the approach in eq 12, the CI coefficients need to be obtained from test simulations with a full set of virtual orbitals for the appropriate intensities and polarization directions of the laser pulse.

A similar approach can be used to determine how many occupied orbitals need to be included:

https://doi.org/10.1021/acs.jpca.4c01732
J. Phys. Chem. A XXXX, XXX, XXX−XXX

$$\text{ratio}(t, i_{\min}) = \frac{\sum_a^{\text{all}} \sum_{i=i_{\min}}^{n_{\text{occ}}} |c_i^{a*}(t) c_0(t) \langle \psi_i^a | \hat{\mathbf{V}}^{\text{abs}} | \psi_0 \rangle| + \sum_{j,a,b}^{\text{all}} \sum_{i=i_{\min}}^{n_{\text{occ}}} |c_i^{a*}(t) c_j^b(t) \langle \psi_i^a | \hat{\mathbf{V}}^{\text{abs}} | \psi_j^b \rangle|}{\sum_a^{\text{all}} \sum_{i=1}^{n_{\text{occ}}} |c_i^{a*}(t) c_0(t) \langle \psi_i^a | \hat{\mathbf{V}}^{\text{abs}} | \psi_0 \rangle| + \sum_{j,a,b}^{\text{all}} \sum_{i=1}^{n_{\text{occ}}} |c_i^{a*}(t) c_j^b(t) \langle \psi_i^a | \hat{\mathbf{V}}^{\text{abs}} | \psi_j^b \rangle|} \tag{15}$$

For TD-CIS simulations, the number of occupied orbitals contributing to the rate can be readily deduced from the orbital energies, since low-lying orbitals do not contribute significantly to the rate. For TD-CISD-IP simulations, the configurations involve two occupied orbitals (one ionized and one excited). While only the orbitals with higher energies will be easily ionized, more occupied orbitals may be excited since these excitations serve to relax the electronic structure of the cation as well as model the ionization of the cation to the dication.

The one-electron density can also be used to estimate the maximum number of virtual orbitals that need to be included. The rate in terms of the density matrix in the molecular orbital basis is

$$\text{rate}(t) = 2 \sum_{p,q}^{\text{all}} \rho_{pq}(t) \langle \phi_p | \hat{\mathbf{V}}^{\text{abs}} | \phi_q \rangle \tag{16}$$

Provided that the molecular orbitals are ordered in terms of increasing energy, the number of virtual orbitals, $a_{\max}$, required for 99% of the full ionization rate can be obtained from the following ratio:

$$\text{ratio}(t, a_{\max}) = \frac{\sum_{p,q}^{a_{\max}} |\rho_{pq}(t) \langle \phi_p | \hat{\mathbf{V}}^{\text{abs}} | \phi_q \rangle|}{\sum_{p,q}^{\text{all}} |\rho_{pq}(t) \langle \phi_p | \hat{\mathbf{V}}^{\text{abs}} | \phi_q \rangle|} \tag{17}$$

Since the individual contributions to the sum can be positive or negative, the absolute values need to be used in calculating the ratio. The values from eq 17 are larger by 10−20 orbitals than $a_{\max}$ calculated with eq 14.

e. Perturbation Theory to Estimate Contribution of Virtual Orbitals to the Ionization Rate. The approaches outlined above require a collection of test simulations with the full set of virtual orbitals and excited states. Since this may not be practical for larger cases, it would be best if the range of orbitals could be estimated before the simulation. As described in the Results and Discussion, tests with the above approach indicate that a static field gives a good estimate of the range of virtual orbitals required for simulating strong field ionization with a variety of linear and circularly polarized pulses. A static field distorts the electron density, and this distortion can be estimated by second-order perturbation theory. In terms of the unperturbed occupied and virtual molecular spin-orbitals ϕ_i and ϕ_a, the perturbed occupied orbitals $\tilde{\phi}_i$ in a field of $E_{\max}$ in the x direction are

$$\tilde{\phi}_i = \sum_p^{\text{all}} d_{ip}^x \phi_p \tag{18}$$

where

$$d_{ij}^x = \delta_{ij}, \quad d_{ia}^x = \frac{E_{\max} D_{a,i}^x}{\Delta\varepsilon}; \quad D_{p,q}^x = \langle \phi_p | \hat{\mu}_i | \phi_q \rangle$$

$$\Delta\varepsilon = \begin{cases} \varepsilon_a - \varepsilon_i & \text{for CIS} \\ \varepsilon_a - \varepsilon_i + \langle ix||ix\rangle - \langle ax||ax\rangle & \text{for CISD-IP} \end{cases}$$

where ε_i and ε_a are the energies of the unperturbed occupied and virtual orbitals, respectively, and the two-electron integrals account for ionization from orbital x for CISD-IP. To incorporate the different polarization directions, the root-mean-square average of the changes in the orbitals is used to estimate the ionization rate:

$$\bar{d}_{ip} = \sqrt{[(d_{ip}^x)^2 + (d_{ip}^y)^2 + (d_{ip}^z)^2]/3} \tag{19}$$

The rate can be written in terms of the electron density and the matrix elements of the absorbing potential in terms of the unperturbed molecular orbitals, ϕ_p.

$$\text{estimated rate} = 2 \sum_i^{\text{occ}} \langle \tilde{\phi}_i | \hat{\mathbf{V}}^{\text{abs}} | \tilde{\phi}_i \rangle = 2 \sum_i^{\text{occ}} \sum_{p,q}^{\text{all}} \bar{d}_{ip}^* \bar{d}_{iq} \langle \phi_p | \hat{\mathbf{V}}^{\text{abs}} | \phi_q \rangle \tag{20}$$

Similar to eq 14, the following ratio is used to estimate the number of virtual orbitals, $a_{\max}$, needed to obtain 99% of the full ionization rate:

$$\text{ratio}(a_{\max}) = \frac{\sum_{p,q}^{a_{\max}} \sum_i^{\text{occ}} |\bar{d}_{ip}^* \bar{d}_{iq} \langle \phi_p | \hat{\mathbf{V}}^{\text{abs}} | \phi_q \rangle|}{\sum_{p,q}^{\text{all}} \sum_i^{\text{occ}} |\bar{d}_{ip}^* \bar{d}_{iq} \langle \phi_p | \hat{\mathbf{V}}^{\text{abs}} | \phi_q \rangle|} \tag{21}$$

In the Results and Discussion, this is termed the perturbation theory (PT) method.

In cases where the perturbational approach has difficulties, the approximate changes in the occupied orbitals can be obtained by diagonalizing the field-free Fock matrix plus the perturbing field (this corresponds to infinite-order perturbation):

$$\sum_q (\varepsilon_p \delta_{pq} - E_{\max} D_{p,q}) d_{iq} = \tilde{\varepsilon}_i d_{ip} \tag{22}$$

The changes in the orbitals could be obtained by performing a full SCF calculation in a finite field and projecting the orbitals in the field onto the field-free orbitals. However, considerable caution is needed to ensure that the orbitals in the field retain the character of the field-free occupied orbitals rather than placing substantial electron density outside the molecular Coulomb well.

f. Natural Orbitals to Calculate the Ionization Rate. An alternative approach to reducing the number of virtual orbitals included in the TD-CI simulation is to adapt the molecular orbitals to the strong field ionization process using a natural orbital approach. This is in the spirit of perturbation-aware pair natural orbitals used to improve the efficiency of calculating response properties with coupled cluster methods (see ref 46 and references therein). Natural orbitals, $\tilde{\tilde{\phi}}$, are obtained by diagonalizing the one-electron density matrix. An average density matrix $\bar{\rho}$ representative of strong field ionization can be obtained by sampling the time-dependent density matrix $\rho(t)$ in a test TD-CI simulation at suitable time intervals and for an appropriate collection of directions:

https://doi.org/10.1021/acs.jpca.4c01732
J. Phys. Chem. A XXXX, XXX, XXX−XXX

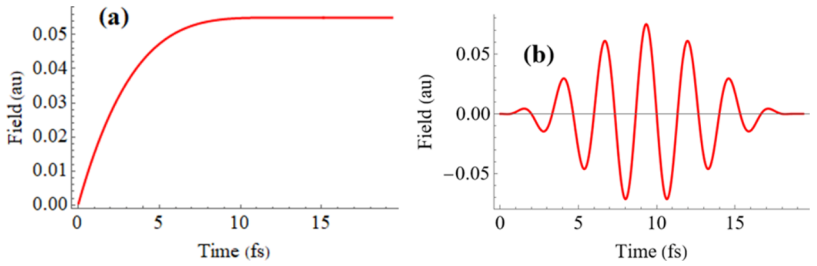

Figure 1. Electric field for (a) a "static" pulse and (b) a seven-cycle 800 nm linearly polarized pulse with a carrier envelope phase of 0° (0.05 au electric field = 2.57 V/Å corresponds to an intensity of 0.88×10^{14} W cm^{-2}). Adapted from ref 36. Copyright 2023 American Chemical Society.

$$\overline{\rho}_{pq} = \frac{1}{n_{\text{sample}}} \sum_{k}^{n_{\text{sample}}} \rho_{pq}(t_k) = \sum_{m}^{\text{all}} n_m e^{*}_{mp} e_{mq}; \qquad \approx{\phi}_m = \sum_{p}^{\text{all}} e_{mp} \phi_m \tag{23}$$

where n_m are the occupation numbers and e_{mp} are the coefficients of the natural orbitals in terms of the canonical molecular orbitals (eigenvalues and eigenvectors of $\overline{\rho}$, respectively). The corresponding average rate can be written in terms of the natural orbitals:

$$\text{average rate} = 2 \sum_{p,q}^{\text{all}} \overline{\rho}_{pq} \langle \phi_p | \hat{\mathbf{V}}^{\text{abs}} | \phi_q \rangle = 2 \sum_{m}^{\text{all}} \overline{n}_m \langle \approx{\phi}_m | \hat{\mathbf{V}}^{\text{abs}} | \approx{\phi}_m \rangle \tag{24}$$

Like eq 21, the following ratio can be used to determine the number of natural orbitals that need to be included to obtain 99% of the ionization rate:

$$\text{ratio}(m_{\max}) = \frac{\sum_{m}^{m_{\max}} n_m \langle \approx{\phi}_m | \hat{\mathbf{V}}^{\text{abs}} | \approx{\phi}_m \rangle}{\sum_{m}^{\text{all}} n_m \langle \approx{\phi}_m | \hat{\mathbf{V}}^{\text{abs}} | \approx{\phi}_m \rangle} \tag{25}$$

In the Results and Discussion, this is termed the natural orbital (NO) method. To take advantage of the reduction in the number of orbitals afforded by the natural orbital approach, the one- and two-electron integrals required for the TD-CI simulation need to be transformed to the natural orbital basis. The TD-CI simulation can then proceed in the same fashion as with the canonical molecular orbitals (note that the Fock matrix is not diagonal in the natural orbital basis). The full implementation and testing of this approach will be undertaken in a future study.

RESULTS AND DISCUSSION

A set of molecules of increasing size has been selected to illustrate potential savings for the approaches discussed in Methods: bromomethane, iodoacetylene, propiolic acid, and benzene. The strong field ionizations of halomethanes were simulated by TD-CIS in an early study.[37] Strong field ionization and charge migration in iodoacetylene have been investigated both experimentally[47] and theoretically.[35,36,48−50] Recent computational studies[51−53] indicate that charge migration in propiolic acid cation may have a longer coherence time than that in iodoacetylene cation. Attosecond electron correlation in benzene cation and dication has been studied by angular streaking.[54]

Previous studies have shown that the strong field ionization rate depends markedly on the relative orientation of the molecule and the polarization direction of the laser pulse.[15,16,27−37] We have probed this angular dependence using a "static" pulse shown in Figure 1a, in which the electric field rises to a constant value. A seven-cycle 800 nm linearly polarized pulse shown in Figure 1b has been used to model more typical strong field ionization processes.

The angular dependence of the instantaneous ionization rate for bromomethane, iodoacetylene, propiolic acid, and benzene is illustrated in Figure 2. The ionization rate is plotted radially, and the angle corresponds to the orientation of the electric field and the direction of the ejected electron. The three-dimensional shape of the strong field ionization rate depends

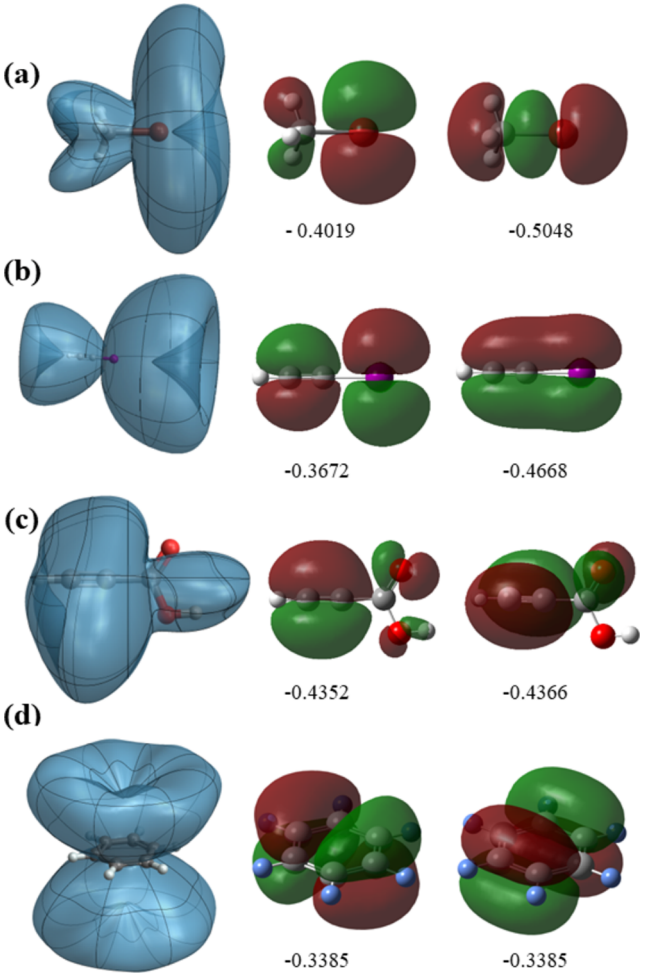

Figure 2. Angular dependence of the instantaneous ionization rate, highest-energy occupied molecular orbital, and second-highest-energy occupied molecular orbital for (a) CH_3Br, (b) HCCI, (c) $HC{\equiv}CCO_2H$, and (d) C_6H_6 (orbital energies in hartree, 1 hartree = 27.211 eV). Panel (b) adapted from ref 36. Copyright 2023 American Chemical Society.

https://doi.org/10.1021/acs.jpca.4c01732
J. Phys. Chem. A XXXX, XXX, XXX−XXX

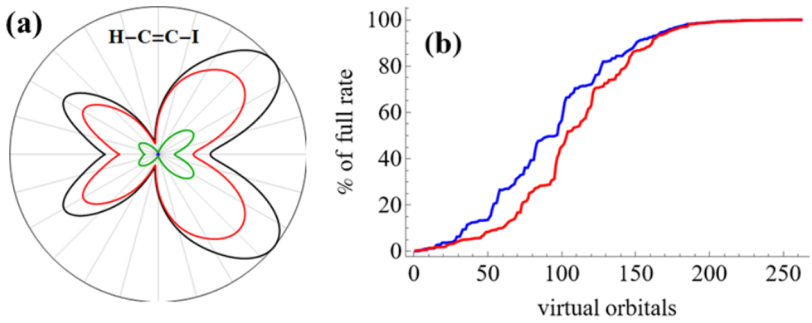

Figure 3. (a) Orbital contributions to the strong field ionization rate for iodoacetylene[35] (total, black; π^*, red; π, green; σ, blue). (b) Cumulative contribution to the total ionization rate as a function of the number of virtual orbitals calculated with the CMO method (eq 14, red) and the PT method (eq 21, blue). Panel (a) adapted from ref 36. Copyright 2023 American Chemical Society.

Table 1. Maximum Number of Virtual Orbitals Needed to Obtain an Estimated 99% of the Total Rate with a 3.0 hartree Cutoff Using a Static Pulse

molecule[a]	3.0 hartree cutoff	CMO method (eq 14)	PT method (eq 21)	NO method (eq 25)
CH_3Br (E_{max} = 0.045 au)	301	232	222	227
CH_3Br^+ (E_{max} = 0.080 au)	301	270	227	187
HCCI (E_{max} = 0.035 au)	262	201	195	213
$HCCI^+$ (E_{max} = 0.060 au)	262	246	199	206
$HCCCO_2H$ (E_{max} = 0.050 au)	301	222	216	198
$HCCCO_2H^+$ (E_{max} = 0.090 au)	301	270	228	235
C_6H_6 (E_{max} = 0.035 au)	450	291	282	216

[a]Numbers of occupied/virtual orbitals in the full simulations after linear dependences and some of the highest-energy virtual orbitals have been removed: 5/319 for CH_3Br, 5/281 for HCCI, 6/352 for propiolic acid, and 5/559 for benzene

on the nodal structure of one or two of the highest-energy occupied molecular orbitals (also shown in Figure 2).

The occupied orbital contributions to the instantaneous ionization rate for iodoacetylene are shown in Figure 3a.[35,36] The highest-energy occupied orbital for HCCI is a π^* orbital and accounts for approximately 80% of the ionization for a field strength of 1.70 V/Å. The second-highest-energy orbital is a π orbital and contributes about 20%. Strong field ionization from the next orbital (σ) is negligible since it lies 0.1 hartree lower in energy than the π orbital. In the TD-CI approach, the rate is obtained from the matrix elements of the absorbing potential with the excited configurations in the time-dependent wavefunction (eq 12). The number of singly excited configurations depends on the number of occupied orbitals times the number of virtual orbitals. For HCCI, an energy cutoff of 3.0 hartree reduces the number of virtual orbitals from 281 to 262. The red curve in Figure 3b shows the number of virtual orbitals interacting significantly with the absorbing potential and contributing the ionization rate for a laser field directed at 45° to the molecular axis. Based on the canonical molecular orbital (CMO) method (eq 14), only 201 virtual orbitals are needed to achieve 99% of the rate obtained with 262 virtual orbitals. The perturbation theory (PT) method (eq 21) is a simpler, less costly estimate of the contributions of the virtual orbitals to the ionization rate and yields a curve similar to that with the CMO method.

Table 1 compares the 3.0 hartree cutoff and the CMO, PT, and NO methods (eqs 14, 21, and 25, respectively) for estimating the number of virtual orbitals interacting significantly with the absorbing potential in order to obtain 99% of the rate from a full simulation. Bromomethane, iodoacetylene, propiolic acid, and benzene are chosen as test cases. The CIS wavefunction is used for the neutral molecules, and the CISD-IP wavefunction is used for the cations. The 3.0 hartree cutoff produces negligible change in the rate but reduces the number of virtual orbitals by 5−20% compared to the full simulation (aug-cc-pVTZ + diffuse basis functions with linear dependences and some of the highest-energy virtual orbitals removed). The greater savings are seen for the larger molecules, which proportionally have more diffuse functions. For 20% reduction in the number of virtual orbitals, the cost of propagating the TD-CI wavefunction is 64% of the original, and the cost of the initial, one-time diagonalizations and matrix multiplications is 50% of the original.

For the CMO, PT, and NO methods, the number of virtual orbitals needed to obtain 99% of the rate was calculated as the maximum number for all time steps and for a full range of directions (e.g., every 30° in θ and ϕ). The CMO method (eq 14) is the most direct approach for determining the contributions of virtual orbitals to the calculation of the ionization rate. Relative to the 3.0 hartree cutoff, the further reduction in the number of virtual orbitals needed to obtain 99% of the rate ranges from 20% to 35% for neutral molecules and from 5% to 10% for cations. The cations require 20% more virtual orbitals than the neutral molecules because the valence electrons in the cations are held more tightly because of the overall positive charge. Consequently, higher field strengths and more virtual orbitals are needed for a similar rate of strong field ionization. While the CMO method is the most robust way of determining the number of virtual orbitals needed, it requires a full simulation of the ionization rate for each of the directions of interest. An alternate, less demanding approach uses second-order perturbation theory to provide an estimate of the contributions of the virtual orbitals to the rate. Compared to the CMO method, the PT estimates (eq 21) for the maximum number of virtual orbitals are about 5% lower for neutral molecules and 15−20% lower for cations. A good estimate of the upper bound of the number of virtual orbitals

https://doi.org/10.1021/acs.jpca.4c01732
J. Phys. Chem. A XXXX, XXX, XXX−XXX

needed is to adjust the PT method by increasing the PT values by 10% for neutral molecules and by 25% for cations. The advantage of using the PT method is that this estimate can be calculated before the expensive diagonalization of the full Hamiltonian. If needed, the required number of virtual orbitals can be reduced further by applying the NO method after the adjusted PT approach.

Depending on the system, a greater reduction in the number of virtual orbitals may be obtained by using natural orbitals. For CH_3Br^+, $HCCI^+$, and benzene, the number of natural orbitals needed (eq 25) is about 10% lower than that estimated by the CMO method (eq 14). However, considerably more effort is needed to carry out TD-CI simulations using natural orbitals. The natural orbitals must be obtained from simulations for a range of directions. Then the two-electron integrals need to be transformed to the natural orbital basis for the TD-CI simulations.

The actual errors in the final rate for a static pulse in a selected direction are given in Table 2 using the maximum

Table 2. Percentage Errors in the Final Rate Compared to the Full Simulation Using a Static Pulse in a Selected Direction[a]

molecule[a]	3.0 hartree cutoff	CMO method	adjusted PT method[b]
CH3Br (E_{max} = 0.045 au)	0.0	−0.5	0.7
CH_3Br^+ (E_{max} = 0.080 au)	0.3	5.7	0.7
CH_3Br^+ (E_{max} = 0.080 au) scaled[c]	0.2	−0.7	0.5
HCCI (E_{max} = 0.035 au)	0.0	0.5	1.0
$HCCI^+$ (E_{max} = 0.060 au)	0.5	2.5	1.7
$HCCI^+$ (E_{max} = 0.060 au) scaled[c]	−0.4	−0.4	−0.5
$HCCCO_2H$ (E_{max} = 0.050 au)	0.0	1.6	0.8
$HCCCO_2H^+$ (E_{max} = 0.070 au)	2.4	6.3	1.9
$HCCCO_2H^+$ (E_{max} = 0.070 au) scaled[c]	−0.2	0.8	0.4
C_6H_6 (E_{max} = 0.035 au)	0.0	0.5	0.4

[a]$\theta = 30°$, $\phi = 30°$ relative to the molecular symmetry axis for CH_3Br, HCCI, and C_6H_6 and relative to the C≡C triple bond for $HCCCO_2H$; since the π_x and π_y ground states of CH_3Br^+ and $HCCI^+$ are degenerate, the initial state is chosen as $\pi_x + i\pi_y$. [b]PT method from Table 1 plus 10% for neutral molecules and plus 25% for cations. [c]Scaled by $\exp(-\alpha\cdot IP_{full})/\exp(-\alpha\cdot IP)$, $\alpha = 0.85$; see the text for discussion.

numbers of virtual orbitals listed in Table 1. The direction ($\theta = 30°$, $\phi = 30°$ relative to the molecular symmetry axis) is chosen so that the rate and the potential error in the rate are relatively large. The main effect of reducing the number of virtual orbitals is to remove the higher-energy orbitals that do not interact significantly with the absorbing potential and do not contribute significantly to the total ionization rate. For the neutral molecules, the errors in the rates compared to the full simulations are less than 1% for each of the three estimates. Reducing the number of virtual orbitals also has a small effect on the energies of the excited states. For neutral HCCI, the lowest 15 states retained their character and had energies within 0.15 eV of the full calculation. The indirect effect of changes in the energy spectrum on the rate is small, since the errors remain within the 1% target. For the cations, there is an additional factor affecting the rates that cannot be readily included in the CMO and PT estimates. For a neutral molecule calculated with a CIS wavefunction, the ground-state energy and its ionization potential do not depend on the number of virtual orbitals. However, for a cation calculated with a CISD-IP wavefunction, the energy of the ground state depends on the number of single excitations. Reducing the number of virtual orbitals leads to fewer single excitations that can stabilize the ground state, resulting in a small increase in the energy of the ground state of the cation. This reduces the ionization potential and produces a corresponding increase in the ionization rate. The resulting errors can be greater than the 1% target. From experiment and approximate theories such as ADK,[7] it is well-known that the strong field ionization rates depend exponentially on the ionization potential (IP), e.g., rate $\approx \exp(-\alpha\cdot IP)$. The dependence of the calculated rate on the change in the ionization potential can be taken into account by scaling the rate by the ratio of exponentials, $\exp(-\alpha\cdot IP_{full})/\exp(-\alpha\cdot IP)$, where $\alpha = 0.85$ is an adjustable parameter. The scaled rates reflect the effect of changing the number of virtual orbitals without changing the ionization potential. The errors in the scaled rates are within the 1% target and are a measure of how well the virtual orbitals interact with the absorbing potential during the simulation. Most simulations compare relative rates (e.g., for different field directions, pulse shapes, pump−probe delays, etc.) rather than absolute rates. The relative rates should not be affected by the weak dependence of the ionization potential on the number of virtual orbitals as long as the simulations use the same number of virtual orbitals and the number is sufficient to interact properly with the absorbing potential.

The effect of field strength on the number of virtual orbitals needed for simulating strong field ionization is shown in Table 3 using iodoacetylene as an example. For field strengths that

Table 3. Maximum Numbers of Virtual Orbitals Needed to Obtain 99% Of the Total Strong Field Ionization Rate for Iodoacetylene with a Static Pulse As a Function of the Field Strength and the Molecular Charge

molecule	CMO method (eq 14)	PT method (eq 21)	NO method (eq 25)
HCCI (E_{max} = 0.030 au)	215	195	245
HCCI (E_{max} = 0.035 au)	215	195	227
HCCI (E_{max} = 0.040 au)	215	195	191
$HCCI^+$ (E_{max} = 0.055 au)	246	199	213
$HCCI^+$ (E_{max} = 0.060 au)	246	199	213
$HCCI^+$ (E_{max} = 0.065 au)	246	199	205

give a reasonable amount of strong field ionization (0.5 to 0.7 for norm^2 at the end of the simulation), little or no difference is seen in the number of virtual orbitals needed. While the results for the CMO and NO methods can depend on the field strength used in the simulation, the PT method (eq 21) is independent of field strength since E_{max} in the numerator and the denominator cancel.

While a static pulse (Figure 1a) is useful in mapping out the angular dependence of the strong field ionization rate (Figure 2), experimental strong field studies typically use few-cycle pulses at 800 nm that are linearly or circularly polarized. Table 4 shows the results with the pulse shown in Figure 1b, a seven-cycle 800 nm pulse with a sin^2 envelope and a carrier envelope phase of 0°. HCCI is used as an example, and the results are for the maximum number of virtual orbitals needed to recover at least 99% of the ionization over a range of directions (every 30° in θ and ϕ). The values for linear and circular polarization are the same as a result of sampling the full range of

https://doi.org/10.1021/acs.jpca.4c01732
J. Phys. Chem. A XXXX, XXX, XXX−XXX

Table 4. Maximum Numbers of Virtual Orbitals Needed to Obtain 99% of the Total Rate for Linearly and Circularly Polarized Seven-Cycle 800 nm $\sin^2$ Pulses

molecule	CMO method (eq 14)	PT method (eq 21)	NO method (eq 25)
HCCI (linear, E_{max} = 0.060)	229	195	241
HCCI (circular, E_{max} = 0.060)	215	195	224
$HCCI^+$ (linear, E_{max} = 0.100)	246	199	238
$HCCI^+$ (circular, E_{max} = 0.100)	246	199	230

polarization directions. For neutral HCCI and the CMO method, the numbers are somewhat larger than for a static pulse. The PT method does not depend on the pulse shape or the field strength. The maximum numbers of virtual orbitals obtained from the NO approach are similar to the values obtained from the CMO approach. Another important aspect of our natural orbital approach illustrated by Table 3 is that natural orbitals seem to perform better at higher field strengths. This is a result of the sampling process used to generate the natural orbitals. Density matrices sampled at higher field strengths have more population in orbitals that overlap with $\mathbf{V}^{abs}$, and the resultant natural orbitals are more strongly adapted to the wavefunction's response to the field. The natural orbital approach also seems to perform better in the cation calculations. This is likely because the natural orbitals were obtained from the cation densities while the canonical orbitals are for the neutral molecule.

As illustrated in Figure 2, the strong field ionization rate depends markedly on the direction of the field relative to the orientation of the molecule. This is governed by the nodal structure of a few of the highest-energy occupied molecular orbitals. As shown in Table 5 for selected directions, the number of virtual orbitals contributing to the ionization rate can be much smaller for a single direction than for the broad range of directions examined in Tables 1, 3, and 4. This could be useful for studying the effect of pulse shape, pulse length, and carrier envelope phase for a given direction or for simulations that vary the delay between pump and probe pulses for a selected direction (see ref 54 for an example). For the CMO method, the maximum number of orbitals needed was obtained from one simulation in a single direction. For the PT approach, the coefficients for the selected direction were used instead of the root-mean-square average of the coefficients obtained with the x, y, and z components of the dipole moment. The natural orbitals were calculated from the average density for a simulation in the selected direction. For a circularly polarized pulse, the directions are sampled from the rotating electric field. The decrease in the number of orbitals needed for simulations in a single direction is a result of various matrix elements of the absorbing potential and dipole moment being zero by symmetry. To benefit from this, the orbitals contributing to the rate can be sorted and the zero contributions eliminated. The example of HCCI shows that this dramatically lowers the number of orbitals compared to the unsorted virtual orbitals. The fewest orbitals are needed for 0° and 180°, followed by 90° and by 45° and 135°. For a circularly polarized pulse (e.g., the electric field rotating in a plane containing the molecule), an intermediate number of orbitals is required. Similar reductions are seen for the natural orbital approach for 0° and 180°. In these cases, the natural orbitals are specifically adapted for the polarization and electron dynamics caused by the oriented electric field.

Table 5. Numbers of Virtual Orbitals Needed to Obtain 99% of the Total Rate for HCCI for Seven-Cycle $\sin^2$ Linear Pulses with E_{max} = 0.060 au for θ = 0°, 45°, 90°, 135°, and 180° and for a Circular Pulse with θ = 90°

Pulse Polarization and Field Direction	CMO method, unsorted	CMO method, sorted[a]	PT method, sorted[a]	NO method, sorted[a]
linear, θ = 0°	227	125	121	127
linear, θ = 45°	221	179	142	201
linear, θ = 90°	215	169	121	188
linear, θ = 135°	222	182	142	202
linear, θ = 180°	219	125	121	115
circular θ = 90°	215	206	155	203

[a]Orbitals were sorted by contribution to the rate before truncation.

SUMMARY

The cost of TD-CI simulations of strong field ionization depends on the number of configurations, which in turn depends on the number of occupied and virtual orbitals used to construct the configurations. The total number of configurations can be reduced by making use of spin symmetry and by using a cutoff for the energy of the excited configurations. The number of virtual orbitals can be reduced by using a cutoff for the orbital energies or by estimating the contribution of the orbitals to the total ionization rate. The number of virtual orbitals interacting significantly with the absorbing potential during a simulation can be determined from the time-dependent CI coefficients and the matrix elements of the absorbing potential in a set of test simulations. Second-order perturbation theory provides a less expensive method for estimating the number of virtual orbitals needed for a simulation. For neutral molecules, these methods reduce the number of virtual orbitals needed by 20−35% compared to a simple 3 hartree cutoff in the orbital energies. This corresponds to a 30−55% reduction in the cost of propagating the TD-CI wavefunction and an even greater savings in the initial setup of the TD-CI calculations. Since cations have a higher ionization potential, the reduction in the number of virtual orbitals needed for simulations of strong field ionization is smaller, 5−10% compared to a 3 hartree cutoff. Adapting the orbitals to the field by deriving natural orbitals from sampled test simulations can also significantly reduce the number of virtual orbitals needed. This natural orbital approach is particularly effective for ionization of cations, resulting in reductions of more than 20%.

AUTHOR INFORMATION

Corresponding Author

H. Bernhard Schlegel − *Department of Chemistry, Wayne State University, Detroit, Michigan 48202, United States;* orcid.org/0000-0001-7114-2821; Email: hbs@chem.wayne.edu

Author

Andrew S. Durden − *Department of Chemistry, Wayne State University, Detroit, Michigan 48202, United States*

Complete contact information is available at: https://pubs.acs.org/10.1021/acs.jpca.4c01732

https://doi.org/10.1021/acs.jpca.4c01732
J. Phys. Chem. A XXXX, XXX, XXX−XXX

Notes

The authors declare no competing financial interest.

■ ACKNOWLEDGMENTS

This work was supported by a grant from the National Science Foundation (CHE1856437) and U.S. Department of Energy, Office of Science, Basic Energy Sciences (award No. DE-SC0020994). A.S.D. thanks WSU for supplemental support for a postdoctoral fellowship. The authors thank the Wayne State University computing grid for generous amounts of computer time.

■ REFERENCES

(1) Posthumus, J. H. The dynamics of small molecules in intense laser fields. *Rep. Prog. Phys.* **2004**, *67*, 623−665.
(2) Ishikawa, K. L.; Sato, T. A review on ab initio approaches for multielectron dynamics. *IEEE J. Sel. Top. Quantum Electron.* **2015**, *21*, No. 8700916.
(3) Nisoli, M.; Decleva, P.; Calegari, F.; Palacios, A.; Martin, F. Attosecond electron dynamics in molecules. *Chem. Rev.* **2017**, *117*, 10760−10825.
(4) Goings, J. J.; Lestrange, P. J.; Li, X. S. Real-time time-dependent electronic structure theory. *Wiley Interdiscip. Rev.-Comput. Mol. Sci.* **2018**, *8*, No. e1341.
(5) Li, X. S.; Govind, N.; Isborn, C.; DePrince, A. E.; Lopata, K. Real-Time Time-Dependent Electronic Structure Theory. *Chem. Rev.* **2020**, *120*, 9951−9993.
(6) Palacios, A.; Martin, F. The quantum chemistry of attosecond molecular science. *Wiley Interdiscip. Rev.-Comput. Mol. Sci.* **2020**, *10*, No. e1430.
(7) Tong, X. M.; Zhao, Z. X.; Lin, C. D. Theory of molecular tunneling ionization. *Phys. Rev. A* **2002**, *66*, No. 033402.
(8) Tolstikhin, O. I.; Morishita, T.; Madsen, L. B. Theory of tunneling ionization of molecules: Weak-field asymptotics including dipole effects. *Phys. Rev. A* **2011**, *84*, No. 053423.
(9) Krause, P.; Klamroth, T.; Saalfrank, P. Time-dependent configuration-interaction calculations of laser-pulse-driven many-electron dynamics: Controlled dipole switching in lithium cyanide. *J. Chem. Phys.* **2005**, *123*, No. 074105.
(10) Rohringer, N.; Gordon, A.; Santra, R. Configuration-interaction-based time-dependent orbital approach for ab initio treatment of electronic dynamics in a strong optical laser field. *Phys. Rev. A* **2006**, *74*, No. 043420.
(11) Krause, P.; Klamroth, T.; Saalfrank, P. Molecular response properties from explicitly time-dependent configuration interaction methods. *J. Chem. Phys.* **2007**, *127*, No. 034107.
(12) Klinkusch, S.; Saalfrank, P.; Klamroth, T. Laser-induced electron dynamics including photoionization: A heuristic model within time-dependent configuration interaction theory. *J. Chem. Phys.* **2009**, *131*, No. 114304.
(13) Greenman, L.; Ho, P. J.; Pabst, S.; Kamarchik, E.; Mazziotti, D. A.; Santra, R. Implementation of the time-dependent configuration-interaction singles method for atomic strong-field processes. *Phys. Rev. A* **2010**, *82*, No. 023406.
(14) Tremblay, J. C.; Klinkusch, S.; Klamroth, T.; Saalfrank, P. Dissipative many-electron dynamics of ionizing systems. *J. Chem. Phys.* **2011**, *134*, No. 044311.
(15) Krause, P.; Sonk, J. A.; Schlegel, H. B. Strong field ionization rates simulated with time-dependent configuration interaction and an absorbing potential. *J. Chem. Phys.* **2014**, *140*, No. 174113.
(16) Krause, P.; Schlegel, H. B. Angle-dependent ionization of small molecules by time-dependent configuration interaction and an absorbing potential. *J. Phys. Chem. Lett.* **2015**, *6*, 2140−2146.
(17) Chu, X.; Chu, S. I. Time-dependent density-functional theory for molecular processes in strong fields: Study of multiphoton processes and dynamical response of individual valence electrons of N_2 in intense laser fields. *Phys. Rev. A* **2001**, *64*, No. 063404.
(18) Chu, X. Time-dependent density-functional-theory calculation of strong-field ionization rates of H_2. *Phys. Rev. A* **2010**, *82*, No. 023407.
(19) Hellgren, M.; Rasanen, E.; Gross, E. K. U. Optimal control of strong-field ionization with time-dependent density-functional theory. *Phys. Rev. A* **2013**, *88*, No. 013414.
(20) Lopata, K.; Govind, N. Near and above ionization electronic excitations with non-hermitian real-time time-dependent density functional theory. *J. Chem. Theory. Comput.* **2013**, *9*, 4939−4946.
(21) Provorse, M. R.; Isborn, C. M. Electron dynamics with real-time time-dependent density functional theory. *Int. J. Quantum Chem.* **2016**, *116*, 739−749.
(22) Bruner, A.; Hernandez, S.; Mauger, F.; Abanador, P. M.; LaMaster, D. J.; Gaarde, M. B.; Schafer, K. J.; Lopata, K. Attosecond charge migration with TDDFT: Accurate dynamics from a well-defined initial state. *J. Phys. Chem. Lett.* **2017**, *8*, 3991−3996.
(23) Sandor, P.; Sissay, A.; Mauger, F.; Abanador, P. M.; Gorman, T. T.; Scarborough, T. D.; Gaarde, M. B.; Lopata, K.; Schafer, K. J.; Jones, R. R. Angle dependence of strong-field single and double ionization of carbonyl sulfide. *Phys. Rev. A* **2018**, *98*, No. 043425.
(24) Kosloff, R.; Kosloff, D. Absorbing boundaries for wave-propagation problems. *J. Comput. Phys.* **1986**, *63*, 363−376.
(25) Muga, J. G.; Palao, J. P.; Navarro, B.; Egusquiza, I. L. Complex absorbing potentials. *Phys. Rep.* **2004**, *395*, 357−426.
(26) Sommerfeld, T.; Ehara, M. Complex Absorbing Potentials with Voronoi Isosurfaces Wrapping Perfectly around Molecules. *J. Chem. Theory. Comput.* **2015**, *11*, 4627−4633.
(27) Krause, P.; Schlegel, H. B. Angle-dependent ionization of hydrides AH(n) calculated by time-dependent configuration interaction with an absorbing potential. *J. Phys. Chem. A* **2015**, *119*, 10212−10220.
(28) Hoerner, P.; Schlegel, H. B. Angular dependence of strong field ionization of CH_3X (X = F, Cl, Br, or I) using time-dependent configuration interaction with an absorbing potential. *J. Phys. Chem. A* **2017**, *121*, 5940−5946.
(29) Hoerner, P.; Schlegel, H. B. Angular dependence of ionization by circularly polarized light calculated with time-dependent configuration interaction with an absorbing potential. *J. Phys. Chem. A* **2017**, *121*, 1336−1343.
(30) Hoerner, P.; Schlegel, H. B. Angular dependence of strong field ionization of haloacetylenes, HCCX (X = F, Cl, Br, I) using time-dependent configuration interaction with an absorbing potential. *J. Phys. Chem. C* **2018**, *122*, 13751−13757.
(31) Winney, A. H.; Basnayake, G.; Debrah, D. A.; Lin, Y. F.; Lee, S. K.; Hoerner, P.; Liao, Q.; Schlegel, H. B.; Li, W. Disentangling strong-field multielectron dynamics with angular streaking. *J. Phys. Chem. Lett.* **2018**, *9*, 2539−2545.
(32) Lee, M. K.; Hoerner, P.; Li, W.; Schlegel, H. B. Effect of spin-orbit coupling on strong field ionization simulated with time-dependent configuration interaction. *J. Chem. Phys.* **2020**, *153*, No. 244109.
(33) Lee, M. K.; Li, W.; Schlegel, H. B. Angular dependence of strong field sequential double ionization for neon and acetylene simulated with time-dependent configuration interaction using CIS and CISD-IP. *J. Chem. Phys.* **2020**, *152*, No. 064106.
(34) Hoerner, P.; Li, W.; Schlegel, H. B. Sequential double ionization of molecules by strong laser fields simulated with time-dependent configuration interaction. *J. Chem. Phys.* **2021**, *155*, No. 114103.
(35) Schlegel, H. B.; Hoerner, P.; Li, W. Ionization of HCCI neutral and cations by strong laser fields simulated with time dependent configuration interaction. *Front. Chem.* **2022**, *10*, No. 866137.
(36) Schlegel, H. B. Charge Migration in HCCI Cations Probed by Strong Field Ionization: Time-Dependent Configuration Interaction and Vibrational Wavepacket Simulations. *J. Phys. Chem. A* **2023**, *127*, 6040−6050.
(37) Hoerner, P.; Schlegel, H. B. Angular Dependence of Ionization of CH_3X using Time-Dependent Configuration Interaction with an Absorbing Potential. *J. Phys. Chem. A* **2017**, *121*, 5940−5946.

https://doi.org/10.1021/acs.jpca.4c01732
J. Phys. Chem. A XXXX, XXX, XXX−XXX

(38) Sissay, A.; Abanador, P.; Mauger, F.; Gaarde, M.; Schafer, K. J.; Lopata, K. Angle-dependent strong-field molecular ionization rates with tuned range-separated time-dependent density functional theory. *J. Chem. Phys.* **2016**, *145*, No. 094105.
(39) Golubeva, A. A.; Pieniazek, P. A.; Krylov, A. I. A new electronic structure method for doublet states: Configuration interaction in the space of ionized 1h and 2h1p determinants. *J. Chem. Phys.* **2009**, *130*, No. 124113.
(40) Frisch, M. J.; Trucks, G. W.; Scalmani, G.; Cheeseman, J. R.; Li, X.; Bloino, J.; Janesko, B. G.; Marenich, A. V.; Zheng, J.; Lipparini, F.; Jenkins, A. J.; Liu, A.; Liu, H.; Schlegel, H. B.; Scuseria, G. E.; Robb, M. A.; Barone, V.; Petersson, G. A.; Nakatsuji, H.; Mennucci, B.; Adamo, C.; Rega, N.; Caricato, M.; Haratchian, H. P.; Ortiz, J. V.; Pawlowski, F.; Izmaylov, A. F.; Hu, H.; Liao, C.; Sonnenberg, J. L.; Williams-Young, D.; Ding, F.; Gomperts, R.; Egidi, F.; Goings, J.; Peng, B.; Petrone, A.; Henderson, T.; Ranasinghe, D.; Zakrzewski, V. G.; Gao, J.; Zheng, G.; Liang, W.; Hada, M.; Ehara, M.; Toyota, K.; Fukuda, R.; Hasegawa, J.; Ishida, M.; Nakajima, T.; Honda, Y.; Kitao, O.; Nakai, H.; Vreven, T.; Throssell, K.; Montgomery, J. A., Jr.; Peralta, J. E.; Ogliaro, F.; Bearpark, M. J.; Heyd, J. J.; Brothers, E. N.; Kudin, K. N.; Staroverov, V. N.; Keith, T. A.; Kobayashi, R.; Normand, J.; Raghavachari, K.; Rendell, A. P.; Burant, J. C.; Iyengar, S. S.; Cossi, M.; Millam, J. M.; Klene, M.; Cammi, R.; Martin, R. L.; Farkas, O.; Foresman, J. B.; Fox, D. J. *Gaussian Development Version*, rev. J.28+; Gaussian, Inc.: Wallingford CT, 2024.
(41) Dunning, T. H. Gaussian-basis sets for use in correlated molecular calculations. 1. The atoms boron through neon and hydrogen. *J. Chem. Phys.* **1989**, *90*, 1007−1023.
(42) Woon, D. E.; Dunning, T. H., Jr. Gaussian basis sets for use in correlated molecular calculations. III. The atoms aluminum through argon. *J. Chem. Phys.* **1993**, *98*, 1358−1371.
(43) Peterson, K. A.; Shepler, B. C.; Figgen, D.; Stoll, H. On the spectroscopic and thermochemical properties of ClO, BrO, IO, and their anions. *J. Phys. Chem. A* **2006**, *110*, 13877−13883.
(44) Peterson, K. A.; Figgen, D.; Goll, E.; Stoll, H.; Dolg, M. Systematically convergent basis sets with relativistic pseudopotentials. II. Small-core pseudopotentials and correlation consistent basis sets for the post-d group 16−18 elements. *J. Chem. Phys.* **2003**, *119*, 11113−11123.
(45) *Mathematica: Software for Technical Computation*, ver. 12.0; Wolfram Research, Inc.: Champaign, IL, 2019.
(46) D'Cunha, R.; Crawford, T. D. Applications of a perturbation-aware local correlation method to coupled cluster linear response properties. *Mol. Phys.* **2023**, *121*, No. e2112627.
(47) Kraus, P. M.; Mignolet, B.; Baykusheva, D.; Rupenyan, A.; Horný, L.; Penka, E. F.; Grassi, G.; Tolstikhin, O. I.; Schneider, J.; Jensen, F.; et al. Measurement and laser control of attosecond charge migration in ionized iodoacetylene. *Science* **2015**, *350*, 790−795.
(48) Jia, D.; Manz, J.; Yang, Y. De- and recoherence of charge migration in ionized iodoacetylene. *J. Phys. Chem. Lett.* **2019**, *10*, 4273−4277.
(49) Jia, D.; Manz, J.; Yang, Y. Timing the recoherences of attosecond electronic charge migration by quantum control of femtosecond nuclear dynamics: A case study for $HCCI^+$. *J. Chem. Phys.* **2019**, *151*, No. 244306.
(50) Jia, D.; Yang, Y. Systematic investigation of the reliability of the frozen nuclei approximation for short-pulse excitation: The example of $HCCI^+$. *Front. Chem.* **2022**, *10*, No. 857348.
(51) Despré, V.; Golubev, N. V.; Kuleff, A. I. Charge Migration in Propiolic Acid: A Full Quantum Dynamical Study. *Phys. Rev. Lett.* **2018**, *121*, No. 203002.
(52) Dey, D.; Kuleff, A. I.; Worth, G. A. Quantum Interference Paves the Way for Long-Lived Electronic Coherences. *Phys. Rev. Lett.* **2022**, *129*, No. 173203.
(53) Golubev, N. V.; Begušić, T.; Vaníček, J. On-the-Fly Ab Initio Semiclassical Evaluation of Electronic Coherences in Polyatomic Molecules Reveals a Simple Mechanism of Decoherence. *Phys. Rev. Lett.* **2020**, *125*, No. 083001.
(54) Winney, A. H.; Lee, S. K.; Lin, Y. F.; Liao, Q.; Adhikari, P.; Basnayake, G.; Schlegel, H. B.; Li, W. Attosecond Electron Correlation Dynamics in Double Ionization of Benzene Probed with Two-Electron Angular Streaking. *Phys. Rev. Lett.* **2017**, *119*, No. 123201.

https://doi.org/10.1021/acs.jpca.4c01732
J. Phys. Chem. A XXXX, XXX, XXX−XXX